Exchange Coupling in Niobocene Trihydrides, $Nb(C_5H_3RR')_2H_3$, and Their Adducts with Copper Triad Cations, $[\{Nb(C_5H_3RR')_2H_3\}_2M]^+$ (R = R′ = H; R = H, R′= $SiMe_3$; R = R′ = $SiMe_3$; M = Cu, Ag, Au)

Antonio Antiñolo,[†] Fernando Carrillo-Hermosilla,[†] Bruno Chaudret,*[,‡] Mariano Fajardo,[§] Juan Fernández-Baeza,[†] Maurizio Lanfranchi,[⊥] Hans-Heinrich Limbach,[∥] Markus Maurer,[∥] Antonio Otero,*[,†] and Maria Angela Pellinghelli[⊥]

Departamento de Química Inorgánica, Orgánica y Bioquímica, Universidad de Castilla-La Mancha, Campus Universitario, 13071 Ciudad Real, Spain, Laboratoire de Chimie de Coordination du CNRS, 205, Route de Narbonne, 31077 Toulouse Cedex, France, Fachbereich Chemie, Institut für Organische Chemie, Freie Universität Berlin, Takustrasse 3, W-1000, Berlin 33, Germany, Departamento de Química Inorgánica, Universidad de Alcalá, 28871 Alcalá de Henares, Spain, and Dipartamento di Chimica Generale ed Inorganica, Chimica Analitica, Chimica Fisica, Universitá degli Studi di Parma, Centro di Studio per la Strutturistica Diffractometrica del CNR, Vialle delle Scienze 78, I-43100 Parma, Italy

Received May 21, 1996[⊗]

The reactions of $Nb(C_5H_3RR')_2Cl_2$ with Red−Al followed by hydrolysis yield $Nb(C_5H_3RR')_2H_3$ (R = R′ = H, **1**; R = H, R′ = $SiMe_3$, **2**; R = R′ = $SiMe_3$, **3**). These compounds react with Lewis acidic coinage cationic species, namely, $[Cu(MeCN)_4]PF_6$, $AgBF_4$, and "$Au(THT)PF_6$", prepared in situ from AuCl(THT) and $TlPF_6$ in a 2 to 1 ratio to yield the adducts $[\{Nb(C_5H_3RR')_2H_3\}_2M]^+$ (M = Cu, R = R′ = H, **7**; R = H, R′ = $SiMe_3$, **8**; R = R′ = $SiMe_3$, **9**; M = Ag, R = H, R′ = $SiMe_3$, **10**; R = R′ = $SiMe_3$, **11**; M = Au, R = R′ = H, **12**; R = H, R′ = $SiMe_3$, **13**; R = R′ = $SiMe_3$, **14**). Like **1**, but unlike the corresponding tantalum derivatives $Ta(C_5H_3RR')_2H_3$ (R = R′ = H, **4**; R = H, R′ = $SiMe_3$, **5**; R = R′ = $SiMe_3$, **6**), **2** and **3** show exchange couplings in their high-field ^1H NMR spectra due to a hydride tunneling phenomenon. The magnitudes of exchange couplings are larger in the cases of **2** and **3** than in the case of **1** as a result of the decrease of electron density upon increasing the number of $SiMe_3$ substituents on the Cp ring. The addition of a Lewis acidic cation results in the observation of an AB_2 pattern for the hydrides at room temperature, which splits at low temperature into an ABC one in agreement with a fluxional behavior of the cation which binds to two hydrides of each niobium center. The activation energy of these fluxional processes are close to 42−45 kJ·mol^{-1} in the case of Cu adducts, 37 kJ·mol^{-1} in the case of Ag adducts, and 40 kJ·mol^{-1} in the case of Au adducts. The magnitude of exchange couplings is reduced upon addition of copper cation to **1**−**3**, is of the same order of magnitude after addition of a silver cation, and is greatly increased by addition of a gold cation. A model is proposed to explain these variations which involves two isomeric states that are close in energy, one involving two bridging and one terminal hydrides on niobium and one involving one bridging hydride and a dihydrogen molecule. A line shape analysis experiment carried out on **14** allows determination of the parameters of the classical exchange, the coupling constants at various temperatures which reach 550 Hz at 347 K, and the parameters of the quantum mechanical exchange according to our proposed model. The structure of **14** has been studied by X-ray diffraction. The structure has been solved from diffractometer data by Patterson method and refined by blocked full-matrix least squares on the basis of 3082 observed reflections to R and R_w values of 0.0346 and 0.0381, respectively. The structure shows the presence of two bridging hydrides between the niobium and gold atoms; one of them is found close to the terminal hydride.

Introduction

Hydride complexes of transition metals represent one of the most important classes of compounds because of their chemical reactivity and importance in catalysis.[1] However, it has been demonstrated lately that a hydrogen atom can be coordinated to a transition metal through different ways. Hence, in addition to the usual direct link either terminal or bridging, the hydrogen atom can be coordinated through a σ-bond (H−H, dihydrogen complex; H−C−agostic complex; H−ER_3, E = Si, Ge, Sn; etc.).[2] The discovery of dihydrogen coordination has been particularly significant and has led to a wide reexamination of hydride chemistry, in particular as far as their real structure is concerned.[3]

Not long after the initial publication by Kubas of dihydrogen coordination,[3a] a few groups, including ours, reported the anomalous spectroscopic properties of various trihydride derivatives of transition metals.[4−7] Thus, the hydride signals in ^1H NMR of these compounds of ruthenium,[4,5] iridium,[6] or niobium[7]

[†] Universidad de Castilla-La Mancha.
[‡] Laboratoire de Chimie de Coordination du CNRS.
[§] Universidad de Alcalá.
[⊥] Universitá degli Studi di Parma.
[∥] Freie Universität Berlin.
[⊗] Abstract published in *Advance ACS Abstracts,* November 15, 1996.

(1) Hlatky, G. G.; Crabtree, R. H. *Coord. Chem. Rev.* **1985**, *65*, 1.
(2) Crabtree, R. H. *Angew. Chem., Int. Ed. Engl.* **1993**, *32*, 789.
(3) (a) Kubas, G. J. *Acc. Chem. Res.* **1988**, *21*, 120. (b) Crabtree, R. H. *Acc. Chem. Res.* **1990**, *23*, 95. (c) Jessop, P. G.; Morris, R. H. *Coord. Chem. Rev.* **1992**, *121*, 155. (d) Heinekey, D. M.; Oldham, W. J., Jr. *Chem. Rev.* **1993**, *93*, 913.
(4) Paciello, R. A.; Manríquez, J. M.; Bercaw, J. E. *Organometallics* **1990**, *9*, 260.
(5) Arliguie, T.; Chaudret, B.; Devillers, J.; Poilblanc, R. *C. R. Hebd. Séances Acad. Sci.* **1987**, *305-II*, 1523.
(6) Heinekey, D. M.; Payne, N. G.; Shulte, G. K. *J. Am. Chem. Soc.* **1988**, *110*, 2303.

S0020-1669(96)00582-4 CCC: $12.00

exhibited large, temperature dependent H−H coupling constants. In fact these were not the first observations of such behavior since the spectroscopic properties of $Nb(C_5H_5)_2H_3$ (**1**)[8] had been puzzling for some time[8e,9] and since Tebbe had observed in the early 1970s large H−H coupling constants upon adding $AlEt_3$ to **1**.[9b]

However, the quantum mechanical nature of the coupling was recognized by Zilm[10] ane Weitekamp[11] who proposed the existence in these compounds of exchange couplings between two hydrogen atoms. Exchange couplings are known in EPR, but their observation on "heavy" particles such as protons were novel in coordination chemistry. These couplings have now been observed on many different metal trihydride systems, most of which display the same geometry characterized by the constraint and coplanarity of the hydrides.[12,13] Exchange coupling between only two hydrides has been observed in a cooper adduct of $Cp^*RuH_3(PCy_3)$[12a,c] and in a tantalum dihydride,[14] whereas recently the appearance of such couplings was proposed in an osmium trihydride derivative not containing cyclopentadienyl ligands.[15]

The exact physical processes accounting for the observation of the phenomenon, however, still remain open to discussion. Zilm and colleagues have proposed a vibrational model for explaining these couplings,[10] whereas some of us have proposed that rotational tunneling of dihydrogen in a thermally accessible dihydrogen state could account for them.[16] Hence, ab initio calculations show that niobium trihydrides possess a hydrido dihydrogen state almost degenerate in energy, whereas such a state is much higher in energy in the case of tantalum trihydrides.[17] Furthermore, $[CpIrH_3(PR_3)]^+$ was also calculated to display a close in the energy hydrido dihydrogen state,[18a] and a number of ab initio electronic energy calculations using an one-dimensional tunneling model have recently been carried out in metallocenes $[Cp_2MH_3]^{n+}$, M = Mo, W ($n = 1$) and M = Nb, Ta ($n = 0$), establishing that the stability of the η^2-H_2 structure relative to the minimum energy trihydride is the main parameter governing the magnitude of the exchange coupling.[18b]

Several observations of exchange couplings on bis(cyclopentadienyl)niobium trihydride derivatives have been previously reported, among which those bearing electron withdrawing substituents display the largest H−H coupling constants in agreement with the importance of a nearby dihydrogen state.[8e,9,13c] These results were reported by us in a preliminary communication and fully described in this paper.[7]

In search for a chemical discrimination between a purely vibrational mechanism and one implying rotational tunneling of dihydrogen, we considered the addition of Lewis acidic coinage cations to these trihydrides. Such additions were expected to inhibit the vibrational mode at the origin of exchange couplings in Zilm and Heinekey's model.

Several authors have prepared polynuclear systems associating transition metal polyhydrides (Re, Mo, Ru, Rh, Ir, ...) and a coinage cation,[12c,19] particularly relevant compounds being $\{(Cp_2MH_2)_2Cu\}PF_6$ (M = Mo, W) recently reported by Caulton et al.[20]

We describe in this paper the synthesis and spectroscopic properties of substituted niobocene trihydrides and the effect on exchange couplings of the addition of copper, silver, or gold cations to these complexes. Preliminary reports of part of this work have been communicated.[7,21]

Results and Discussion

Preparation and Spectroscopic Properties of Substituted Niobocene Trihydrides $Nb(C_5H_3RSiMe_3)_2H_3$ (R = H, 2; $SiMe_3$, 3). The trihydrides **2** and **3** were prepared like **1** by reaction of $Nb(C_5H_3RSiMe_3)_2Cl_2$ with excess of Red−Al in toluene.[8d] After hydrolysis, evaporation to dryness, and recrystallization from ethanol, **2** and **3** were obtained as white crystalline materials.

The corresponding tantalum trihydrides were prepared similarly according to published procedures to give $Ta(C_5H_3RR')_2H_3$ (R = R′ = H, **4**; R = H, R′ = $SiMe_3$, **5**; R = R′ = $SiMe_3$, **6**). All complexes **1**−**6** show very similar M−H stretching frequencies in infrared (1710−1760 cm^{-1}), but they display very different NMR behaviors. Hence, the tantalum trihydride derivatives show at high field an AB_2 pattern for the hydride ligands with magnetic coupling constants of ca. 10 Hz not dependent upon the temperature as expected (see Experimental Section). The high-field spectra of **1** have been discussed by several authors, including recently Labinger,[9] Curtis,[8e] and Heinekey,[13c] while we have reported those of **2** and **3** in a preliminary form.[7] Compound **1** shows in ^1H NMR two broad signals at high field respectively at δ −2.75 and −3.75. Lowering the temperature leads first to the observation of broad lines and then at very low temperature to the reappearance of

(7) Antiñolo, A.; Chaudret, B.; Commenges, G.; Fajardo, M.; Jalón, F.; Morris, R. H.; Otero, A.; Schweitzer, C. T. *J. Chem. Soc., Chem. Commun.* **1988**, 1210.
(8) (a) Tebbe, F. N.; Parshall, G. W. *J. Am. Chem. Soc.* **1971**, *93*, 3793. (b) Tebbe, F. N. *J. Am. Chem. Soc.* **1973**, *95*, 5142. (c) Wilson, K. D.; Koetzle, T. F.; Hart, D. W.; Kvick, A.; Tipton, D. L.; Bau, R. *J. Am. Chem. Soc.* **1977**, *99*, 1775. (d) Green, M. L. H.; Moreau, J. J. E. *J. Organomet. Chem.* **1978**, *C25*, 161. (e) Curtis, M. D.; Bell, L. G.; Butler, W. M. *Organometallics* **1985**, *4*, 701.
(9) (a) The NMR properties of $Nb(C_5H_5)_2H_3$ were discussed by Labinger: Labinger, J. A. In *Comprehensive Organometallic Chemistry*; Wilkinson, G., Stone, F. G. A., Abel, E. W., Eds.; Pergamon Press: New York, 1983; Vol. 3, p 707. (b) Tebbe, F. N. Cited as unpublished results in ref 9a).
(10) (a) Zilm, K. W.; Heinekey, D. M.; Millar, J. M.; Payne, N. G.; Demou, P. *J. Am. Chem. Soc.* **1989**, *111*, 3088. (b) Zilm, K. W.; Heinekey, D. M.; Millar, J. M.; Payne, N. G.; Neshyba, S. P.; Duchamp, J. C.; Szczyrba, J. *J. Am. Chem. Soc.* **1990**, *112*, 92.
(11) Jones, D.; Labinger, J. A.; Weitekamp, D. P. *J. Am. Chem. Soc.* **1989**, *111*, 3087.
(12) (a) Chaudret, B.; Commenges, G.; Jalón, F.; Otero, A. *J. Chem. Soc., Chem. Commun.* **1989**, 210. (b) Arliguie, T.; Border, C.; Chaudret, B.; Devillers, J.; Poilblanc, R. *Organometallics* **1989**, *8*, 1308. (c) Arliguie, T.; Chaudret, B.; Jalón, F.; Otero, A.; López, J. A.; Lahoz, F. J. *Organometallics* **1991**, *10*, 1888.
(13) (a) Heinekey, D. M.; Harper, T. G. P. *Organometallics* **1991**, *10*, 2891. (b) Heinekey, D. M.; Payne, N. G.; Sofield, C. C. *Organometallics* **1990**, *9*, 2643. (c) Heinekey, D. M. *J. Am. Chem. Soc.* **1991**, *113*, 6074. (d) Heinekey, D. M.; Millar, J. M.; Koetzle, T. F.; Payne, N. G.; Zilm, K. W. *J. Am. Chem. Soc.* **1990**, *112*, 909.
(14) Chaudret, B.; Limbach, H. H.; Moise, C. *C. R. Hebd. Séances Acad. Sci.* **1992**, *315-II*, 533.
(15) Gusev, D. G.; Kuhlman, R.; Sini, G.; Eisenstein, O.; Caulton, K. G. *J. Am. Chem. Soc.* **1994**, *116*, 2685.
(16) Limbach, H. H.; Maurer, M.; Scherer, G.; Chaudret, B. *Angew. Chem.* **1992**, *31*, 1369.
(17) Barthelat, J. C.; Chaudret, B.; Daudey, J. P.; De Loth, P.; Poilblanc, R. *J. Am. Chem. Soc.* **1991**, *113*, 9896.
(18) (a) Jarid, A.; Moreno, M.; Lledós, A.; Lluch, J. M.; Bertrán, J. *J. Am. Chem. Soc.* **1993**, *115*, 5861. (b) Camanyes, S.; Maseras, F.; Moreno, M.; Lledós, A.; Lluch, J. M. *J. Am. Chem. Soc.* **1996**, *118*, 4617.
(19) (a) Mueting, A. M.; Bos, W.; Alexander, B. D.; Doyle, P. D.; Casalnuovo, J. A.; Balaban, S.; Ito, L. N.; Johnson, S. M.; Pignolet, L. H. *New J. Chem.* **1988**, *12*, 505, and references cited therein. (b) Venanzi, L. M. *Coord. Chem. Rev.* **1982**, *43*, 251. (c) Rhodes, L. F.; Huffman, J. C.; Caulton, K. G. *J. Am. Chem. Soc.* **1983**, *105*, 5137. (d) Rhodes, L. F.; Huffman, J. C.; Caulton, K. G. *J. Am. Chem. Soc.* **1985**, *107*, 1759. (e) Soloveichik, G. L.; Bulychev, B. M. *Russ. Chem. Rev.* **1983**, *52*, 43. (f) Albinati, A.; Lehner, H.; Venanzi, L. M.; Wolfer, M. *Inorg. Chem.* **1987**, *26*, 3933.
(20) Rhodes, L. F.; Huffman, J. C.; Caulton, K. G. *Inorg. Chim. Acta* **1992**, 198.
(21) (a) Antiñolo, A.; Carrillo, F.; Fernández-Baeza, J.; Otero, A.; Fajardo, M.; Chaudret, B. *Inorg. Chem.* **1992**, *31*, 5156. (b) Antiñolo, A.; Carrillo, F.; Chaudret, B.; Fajardo, M.; Fernández-Baeza, J.; Lanfranchi, M.; Limbach, H.-H.; Maurer, M.; Otero, A.; Pellinghelli, M. A. *Inorg. Chem.* **1994**, *33*, 5163.

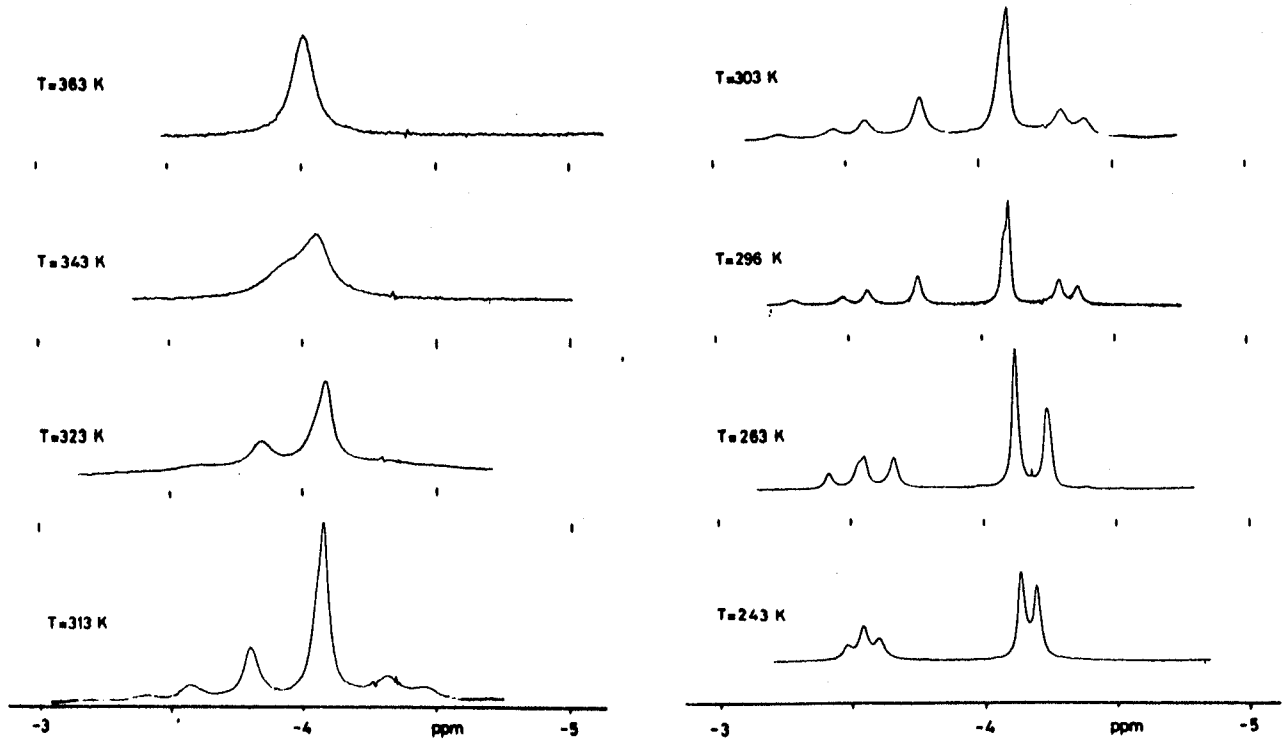

Figure 1. Variation of the high-field ^{1}H NMR spectra of **2** as a function of temperature (250 Mhz, toluene-d_8).

couplings.[13c] This phenomenon was interpreted as due to opposite signs for the exchange and magnetic coupling constants.

In contrast, the niobium complexes **2** and **3** show at room temperature the AB_2 pattern for the hydrides but characterized by large coupling constants (**2**, 36.5 Hz; **3**, 70.0 Hz) which vary with temperature but not with the magnetic field. Figure 1 show the temperature dependence of the NMR spectra of **2**. At 200 K the couplings are not resolved anymore, as for **1** at room temperature. Further lowering of the temperature did not lead to reappearance of the couplings, but this is probably due to the fact that the temperature dependence curve is very flat in this region. The longitudinal relaxation time T_1 of the hydrides was measured for **2**, **3**, and **5**. It was found that all hydrides show the same minimum of 40 and 55 ms (this value should be corrected to 100 ms when the influence of the Nb−H dipole−dipole relaxation is accounted for),[3c] at 205 K, in the case of **3** and **2**, respectively, whereas in the case of **5** two distinct values of 127 (H_A) and 196 ms (H_B) were found. The two values found in the case of **5** clearly demonstrate the lack of exchange between the hydrides in this case, whereas in the case of complex **2** a slow exchange regime is probably still present. The value of 40 ms found for the hydrides of **2** is short but could result from a relaxation process involving the niobium nucleus.

Finally it is noteworthy that the presence of electron withdrawing substituents on the Cp ring strongly influences the magnitude of exchange couplings.

Reactions of Substituted Niobocene Trihydrides (1−3) with Cationic Coinage Metal Complexes (See Scheme 1). Complex **1** reacts at −78 °C, complexes **2** and **3** at room temperature with $[Cu(MeCN)_4]PF_6$ in a 2:1 ratio in THF for 15 min to give colorless or slightly brown solutions, which after appropriate workup yield white, air-sensitive microcrystalline solids of composition $[\{Nb(C_5H_3RR')_2H_3\}_2Cu\}]PF_6$ (R = R′ = H, **7**; R = H, R′ = $SiMe_3$, **8**; R = R′ = $SiMe_3$, **9**) in ca. 90% yield (see Experimental Section). The reaction is selective since, for example, no substitution of hydrides by acetonitrile is observed. Complexes **8**, **9**, and especially **7** are unstable in solution, slowly depositing metallic copper. This lack of stability can result from the possibility of electron transfer between copper and the niobium−hydride moiety and also from the poor stabilization of copper by the four hydrides. All complexes were characterized by microanalytical and spectroscopic data; the latter will be discussed in the following section.

Scheme 1. Reactions of Substituted Niobocene Trihydrides with Lewis Acidic Cations

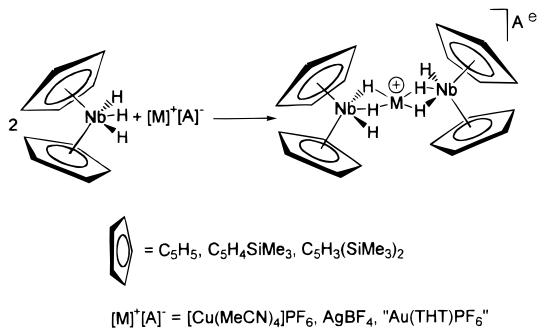

Similar reactions between **1** and **3** and $AgBF_4$ in a 2:1 ratio are rapid at room temperature and lead to red brown solutions (see Scheme 1). In the case of the reaction with **1**, the solution briefly deposits metallic silver, even at low temperature. However, in the case of the reactions of **2** and **3**, appropriate workup leads to the formation of white crystals of $[\{Nb(C_5H_3RR')_2H_3\}_2Ag\}]BF_4$ (R = H, R′ = $SiMe_3$, **10**; R = R′ = $SiMe_3$, **11**). The complexes are both air-sensitive and moderately light and heat-sensitive, depositing silver in both cases, probably again as a result of electron transfer process.

Finally, similar reactions can be carried out between **1**−**3** and "Au(THT)PF_6", prepared in situ by reacting AuCl(THT) with $TlPF_6$ at −78 °C (see Scheme 1). The reactions are carried out in a 2:1 ratio and lead after appropriate workup to pale yellow crystalline materials of stoichiometry $[\{Nb(C_5H_3RR')_2H_3\}_2Au]PF_6$ (R = R′ = H, **12**; R = H; R′ = $SiMe_3$, **13**; R = R′ = $SiMe_3$, **14**). Complexes **12**−**14** were found to be more stable than **7**−**11**. However, again, gold was deposited

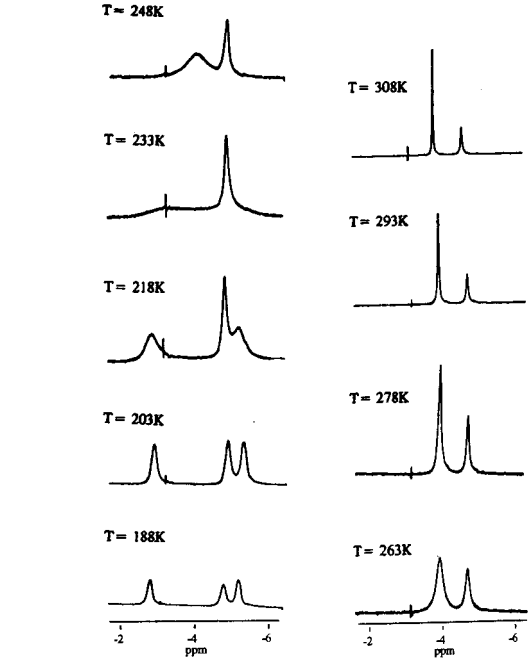

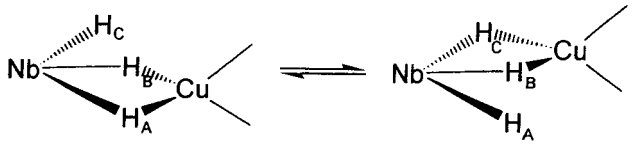

Figure 2. Variation of the high-field ^{1}H NMR spectra of **8** as a function of temperature (250 Mhz, acetone-d_6).

when solutions of **12**−**14** were left at room temperature for several days.

Spectroscopic and Crystallographic Characterization of the Adducts. The cyclopentadienyl ligands C_5H_3RR' display a singlet (R = R′ = H) near 5.5−6.0 ppm, an AA′BB′ (R = H, R′ = $SiMe_3$) near 5.2 and 6.0 ppm, or an AB_2 pattern (R = R′ = $SiMe_3$) near 5.0 and 5.5 ppm. The exact values are given in the Experimental Section but do not appear to show a significant variation with the presence and nature of the Lewis acid. Similarly the $SiMe_3$ groups linked to Cp appears as singlets near 0.0 ppm.

As expected, however, the hydride signals are strongly dependent upon the presence and the nature of the Lewis acid.

Complexes **8** and **9**, formally resulting from the addition of "Cu^+" to **2** and **3**, show two broad singlets for the hydrides in a 2:1 ratio at room temperature, but no observable coupling constant ($w_{1/2}$ respectively 7 and 11 Hz). Lowering the temperature leads to a splitting of the peak of intensity 2 into two new lines of intensity 1 at 235 K for **8** and 220 K for **9** (see Figure 2). This splitting results from the transformation of an AB_2 pattern into an ABC one when the rate of the fluxional process exchanging the two outer hydrides on each niobium center (A and C) is reduced as illustrated on Figure 2. In this case, lowering the temperature down to 188 K did not lead to the reappearance of observable coupling constants. The addition of copper to **2** and **3** therefore leads to a dramatic reduction of the observed H−H coupling constants due probably essentially to a reduction of the exchange coupling constant. However, some quantum mechanical exchange is probably still present since no magnetic coupling is observed. This would be in agreement with Heinekey's proposal that in these systems the exchange and magnetic coupling constants are opposite in sign.[13c]

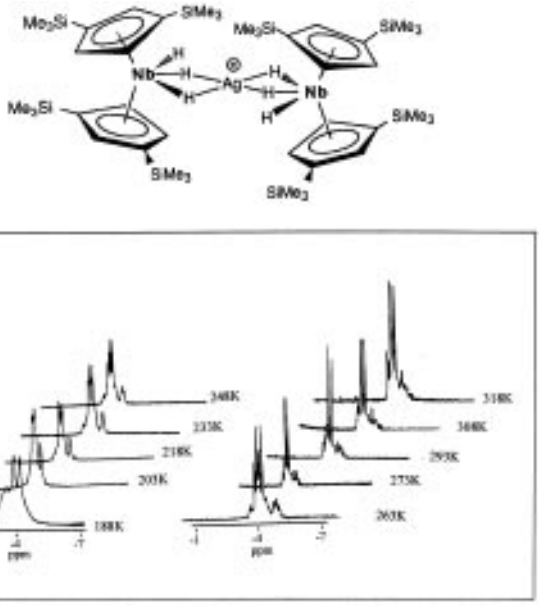

Figure 3. Variation of the high-field ^{1}H NMR spectra of **11** as a function of temperature (250 Mhz, acetone-d_6).

In contrast, the high-field spectrum of **7** shows at room temperature an AB_2 pattern ($\delta_A = -6.2$ and $\delta_B = -4.2$, $J_{AB} = 16$ Hz) in which the lines are sharp. A fluxional process is present as expected since the lines broaden down to 233 K. Two new signals are present at 188 K which were not identified. However, the most salient feature of these spectra is that the H−H coupling constants are not temperature dependent. This indicates that they are usual magnetic coupling constants.

These observations are very meaningful as far as our knowledge of the tunneling process of hydrides is concerned. Hence, they demonstrate that addition of copper displays a "freezing" behavior toward the tunneling process, leading to the observation of usual magnetic couplings; this point will be discussed further in this paper. Furthermore we confirm that exchange and magnetic coupling constants are opposite in sign. The spectra of **8** and **9** suggest that the presence of small exchange coupling constants will lead to unresolved spectra. Hence, the linewidths of the high-field signals of **8** and **9** are respectively 7 and 11 Hz at room temperature (300 MHz in acetone-d_6), whereas it is less than 5 Hz in the case of **7**. The absence of apparent variation of the spectra of **8** and **9** could result from a very low temperature dependence in this array of temperature.

The complex of addition of silver to **1** is unfortunately unstable, and the spectrum of **10** is not informative. Thus, it consists of a broad line at room temperature which splits at low temperature but gives broad superposed features which we found difficult to interpret. However, the high-field spectrum of **11** is quite interesting (Figure 3). Hence, it consists of an AB_2X pattern down to 203 K. A decoalescence of peaks appears on the last spectrum recorded at 188 K. It is possible to deduce from the spectrum at 263 K the different coupling constants J_{H_A-Ag} (37.5 Hz), J_{H_B-Ag} (85.5 Hz), and $J_{H_A-H_B}$ (22 Hz) (see Chart 1). Several pieces of information are accessible from these data. The observation that both the "A" and "B" signals, with $\delta_A = -3.85$ ppm and $\delta_B = -4.25$ ppm, are coupled to silver and that the magnitude of J_{H_A-Ag} is less than half of J_{H_B-Ag} confirms that in solution two hydrides (the B and one of the A) are linked to silver and that a fluxional process renders both H_A equivalents. The second interesting feature is that the silver adducts are more fluxional than their copper counterparts. Finally, the observed values of H−H couplings

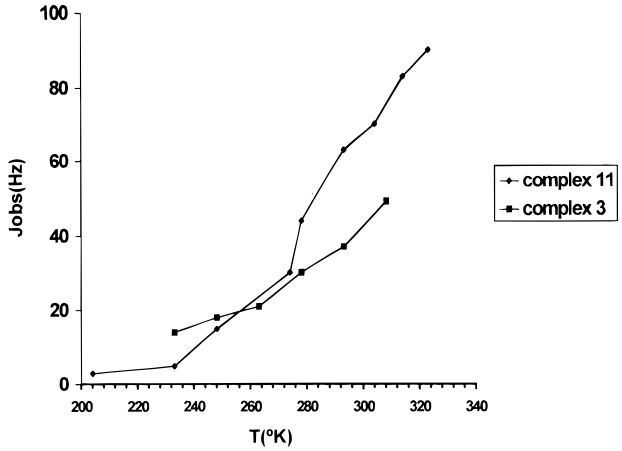

Figure 4. Variation of J_{H-H} as a function of temperature for the hydride signals of **3** and of its adduct **11**.

Chart 1. High-Field ^{1}H NMR Spectrum for Complex **11** at 263 K (250 MHz) and the Proposed Structure in Solution

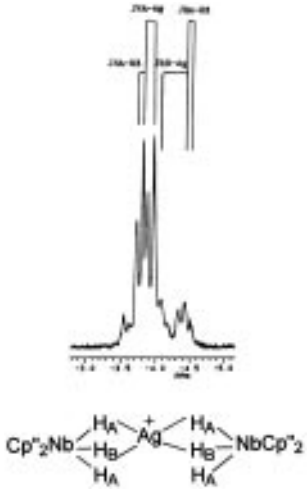

for **11** are similar to those found for the starting complex **3**, but the variation is different (more flat; see Figure 4).

The behavior of the three gold complexes **12**−**14** is clearly different. An AB_2 type pattern is observed at room temperature which splits into an ABC one at low temperature, the coalescence temperature being near 213 K. The spectra of **12** and **14** are clear; that of **13** is more difficult to interpret since the B part of the spectrum is hidden by the Me_3Si signal. It is, however, immediately apparent that in the three systems large H−H coupling constants are present, much larger than in the copper and silver systems, but even than in the starting complexes. An estimation of the variation of the coupling constants with the temperature of **12**−**14** is given in Figure 5.

Since this system displayed an interesting potential for the study of the classical and quantum mechanical processes involved in the adducts, we undertook a study of the behavior of **14** in acetone-d_6, THF-d_8, and a freon mixture.[21]

The spectra of **14** were measured between 198 and 338 K in acetone-d_6, between 200 and 340 K in THF-d_8, and between 140 and 280 K in the freon mixture $CDCl_2F/CDClF_2$. In Figure 6, several experimental and simulated spectra in the commented freon mixture are shown. At low temperature (near 180 K) three signals are present for respectively H_B, H_A, and H_C. H_A and H_B represent the two hydrides linked to gold, whereas the tunneling process occurs between H_B and H_C, both of which

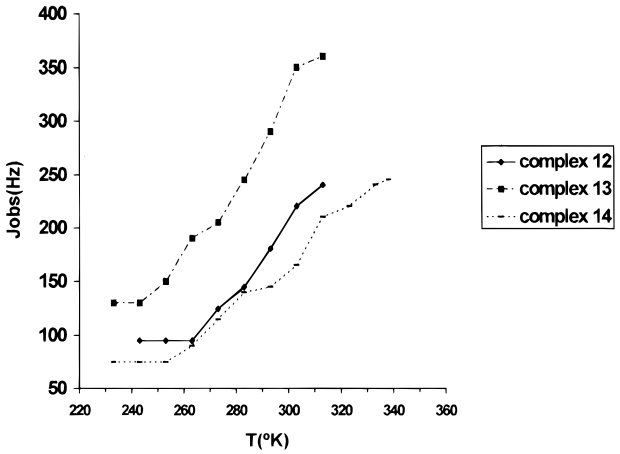

Figure 5. Variation of J_{H-H} as a function of temperature for the hydride signals of **12**−**14**.

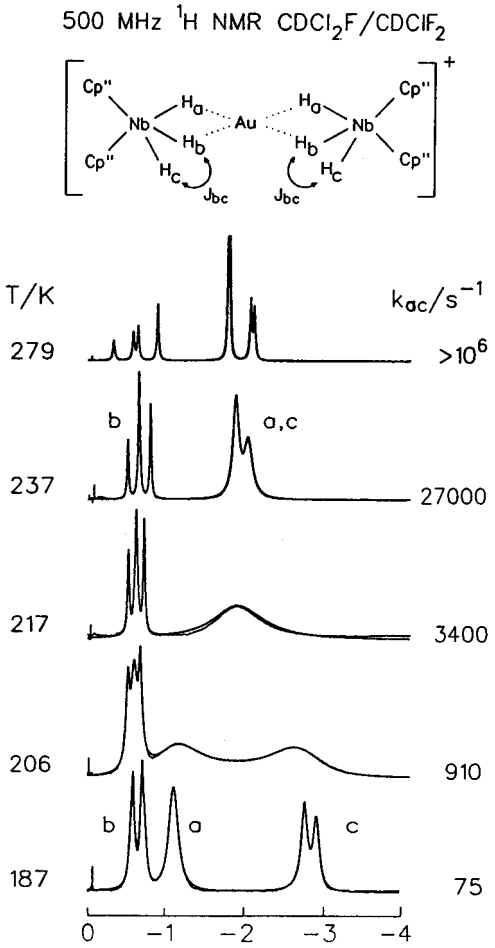

Figure 6. Experimental and simulated spectra for complex **14** in $CDCl_2F/CDClF_2$.

display a temperature dependent doublet. Upon an increase in the temperature, a coalescence occurs near 215 K to give an AB_2 pattern, and another one is apparent above 340 K which will render all hydrides equivalent. By contrast, at temperatures below 180 K, a further splitting of hydride signals occur, which is related to splittings in the A_2B_2 pattern of the cyclopentadienyl protons. It is probable that at these low temperatures the free rotation of the bulky cyclopentadienyl rings is blocked and that we are observing different conformers.

The first clear and unexpected result is the large solvent dependence of the observed H−H coupling constant. For

(22) Hasegawa, T.; Li, Z.; Parkin, S.; Hope, H.; McMullan, R. K.; Koetzle, T. F.; Taube, H. *J. Am. Chem. Soc.* **1994**, *116*, 4352.

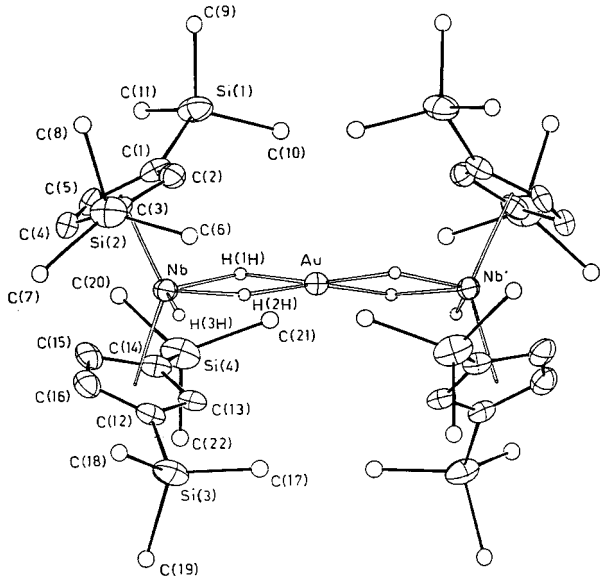

Figure 7. ORTEP view of **14**·3THF. The thermal ellipsoids are drawn at the 30% probability level.

Table 1. Selected Bond Distances (Å) and Angles (deg) for Complex **14**·3THF[a]

	Distances		
Au−Nb	2.965(1)	Nb−H(1H)	1.77(10)
Au−H	1.76(10)	Nb−H(2H)	1.94(10)
Au−H(2H)	1.84(10)	Nb−H(3H)	1.77(10)
Nb−C(1)	2.436(8)	Nb−C(12)	2.456(8)
Nb−C(2)	2.383(9)	Nb−C(13)	2.403(8)
Nb−C(3)	2.417(9)	Nb−C(14)	2.405(9)
Nb−C(4)	2.389(10)	Nb−C(15)	2.401(9)
Nb−C(5)	2.404(9)	Nb−C(16)	2.391(10)
Nb−CE(1)	2.074(9)	Nb−CE(2)	2.082(9)
Si(1)−C(1)	1.884(9)	Si(3)−C(12)	1.882(10)
Si(2)−C(3)	1.870(9)	Si(4)−C(14)	1.894(10)
H(2H)−H(3H)	1.45(14)		
	Angles		
H(2H)−Au−H(2H)′	166(4)	H(2H)−Nb−H(3H)	46(4)
H(1H)−Au−H(2H)′	109(4)	H(3H)−Nb−CE(2)	99(3)
H(1H)−Au−H(1H)′	167(5)	H(1H)−Nb−H(2H)	70(4)
H(1H)−Au−H(2H)	72(4)	H(1H)−Nb−H(3H)	115(5)
Nb−Au−Nb′	175.79(2)	CE(1)−Nb−CE(2)	136.0(3)
H(1H)−Nb−CE(1)	107(3)	Au−H(1H)−Nb	114(5)
H(1H)−Nb−CE(2)	101(3)	Au−H(2H)−Nb	103(5)
H(2H)−Nb−CE(1)	107(3)	Nb−H(2H)−H(3H)	61(6)
H(2H)−Nb−Ce(2)	114(3)	Au−H(2H)−H(3H)	161(8)
H(3H)−Nb−CE(1)	99(3)	Nb−H(3H)−H(2H)	73(6)

[a] The primed atoms are related to the unprimed ones by the transformation $-x, y, {}^1/_2-z$.

example at 278 K, the value of $J_{H_B-H_C}$ is 228 Hz in THF-d_8 an 290 Hz in freon.

This point and the temperature dependence will be discussed hereafter.

In order to determine whether the mode of coordination of gold would be different from that observed for other Lewis acid adducts of polyhydrides, an X-ray crystal structure of **14** was carried out. In the crystals of **14**·$3C_4H_8O$, heterotrinuclear cationic complexes $\{[Nb(C_5H_3(SiMe_3)_2)_2H_3]_2Au\}^+$, PF_6^- anions, and THF molecules of solvation are present. The structure of the cation, having an imposed C_2 symmetry with the Au atom lying on a 2-fold axis, is depicted in Figure 7, together with the atomic numbering scheme; the most important bond distances and angles are given in Table 1, and the atomic coordinates for all non-hydrogen atoms appear in Table 2.

The metal core consists of an almost linear NbAuNb′ arrangement, in which the Nb···Au separation is 2.965(1) Å,

Table 2. Atomic Coordinates ($\times 10^4$) and Isotropic Thermal Parameters ($Å^2 \times 10^4$) with Estimated Standard Deviations in Parentheses for the Non-Hydrogen Atoms of Complex **14**·3THF

atom	*x*	*y*	*z*	*U*
Au	0	1200.8(2)	2500	413(1)[a]
Nb	1655.1(4)	1254.9(4)	2869.3(3)	364(2)[a]
P(1)	5000	628(6)	2500	1641(45)[a]
Si(1)	1633(2)	−502(1)	2042(1)	680(11)[a]
Si(2)	1718(2)	498(2)	4433(1)	696(12)[a]
Si(3)	1314(2)	3034(1)	3559(1)	635(11)[a]
Si(4)	2103(2)	1864(2)	1288(1)	725(13)[a]
F(1)	5650(11)	848(11)	2920(8)	1262(60)
F(2)	4511(11)	450(12)	3076(9)	1367(66)
F(3)	4506(13)	1300(12)	2350(11)	1808(87)
F(4)	4496(18)	−65(16)	2562(18)	2469(141)
F(5)	4415(14)	952(13)	2957(11)	1710(89)
F(6)	4383(16)	188(15)	2112(13)	1966(105)
C(1)	1865(6)	83(4)	2658(4)	499(34)[a]
C(2)	1446(5)	146(4)	3197(4)	455(32)[a]
C(3)	1926(6)	465(4)	3635(4)	468(32)[a]
C(4)	2644(5)	618(5)	3343(5)	494(35)[a]
C(5)	2606(5)	386(5)	2763(5)	490(36)[a]
C(6)	696(8)	739(8)	4558(5)	1164(69)[a]
C(7)	2411(10)	1093(8)	4764(5)	1377(81)[a]
C(8)	1920(11)	−351(7)	4708(6)	1476(91)[a]
C(9)	1522(10)	−1325(5)	2355(6)	1272(72)[a]
C(10)	788(11)	−289(7)	1622(8)	1889(103)[a]
C(11)	2477(14)	−498(10)	1538(9)	2612(155)[a]
C(12)	1775(6)	2459(4)	3012(4)	485(34)[a]
C(13)	1502(5)	2330(4)	2429(4)	462(30)[a]
C(14)	2076(6)	1988(4)	2105(4)	468(32)[a]
C(15)	2728(5)	1884(4)	2486(5)	524(32)[a]
C(16)	2525(5)	2161(5)	3042(5)	505(37)[a]
C(17)	269(8)	3005(8)	3508(8)	1728(98)[a]
C(18)	1634(14)	2837(8)	4309(6)	2020(123)[a]
C(19)	1667(10)	3867(6)	3394(6)	1366(76)[a]
C(20)	2929(8)	1289(9)	1099(6)	1463(82)[a]
C(21)	1155(8)	1546(8)	1000(5)	1152(66)[a]
C(22)	2241(14)	2681(7)	968(6)	1998(126)[a]
C(1A)	3921(26)	2671(24)	4311(20)	1690(163)
C(2A)	4273(30)	3082(23)	3909(21)	1865(168)
C(3A)	5110(32)	2976(25)	4129(22)	2135(190)
C(4A)	4798(38)	2267(27)	4405(24)	2214(225)
C(5A)	4039(29)	2115(24)	4160(20)	1868(166)
C(6A)	4897(30)	2523(23)	3623(22)	2035(183)
C(1B)	372(41)	5009(36)	4568(30)	2564(292)
C(2B)	425(31)	4501(27)	4985(26)	2255(220)
C(3B)	383(38)	5189(31)	5440(28)	2433(254)
CE(1)	2097(5)	340(4)	3119(4)	
CE(2)	2121(5)	2165(4)	2615(4)	

[a] Equivalent isotropic *U* defined as one-third of the trace of the orthogonalized $\mathbf{U}_{ij}$ tensor. CE(1) and CE(2) are the centroids of the cyclopentadienyl rings C(1)−C(5) and C(12)−C(16), respectively.

comparable to that of other niobium gold hydride clusters which lie between 2.99 and 2.91 Å,[23] and the NbAuNb′ angle is 175.79(2)°. The fragment $Nb[C_5H_3(SiMe_3)_2]_2$ adopts the familiar bent sandwich geometry with the two cyclopentadienyl rings coordinated to the metal atom in the η^5-conventional fashion. Three hydrogen atoms, H[1H], H[2H], and H[3H], complete the coordination around the Nb atom [Nb−H[1H] = 1.77(10), Nb−H[2H] = 1.94(10), Nb−H[3H] = 1.77(10) Å]. Moreover, H[1H] and H[2H] make a bridge with the Au atom (Au−H[1H] = 1.76(10), Au−H[2H] = 1.84(10) Å). These data must be taken with care because of the uncertainty in the locations of the hydrogen atoms by X-ray crystallography, even if the same result was obtained from two independent X-ray structure resolutions from two different crystals. The most intriguing geometrical feature of the structure is the presence

(23) Antiñolo, A.; Burdett, J. K.; Chaudret, B.; Eisenstein, O.; Fajardo, M.; Jalón, F.; Lahoz, F.; López, J. A.; Otero, A. *J. Chem. Soc. Chem. Commun.* **1990**, 17.

of two hydrides close to one another (H[2H]−H[3H] = 1.45(14) Å; for comparison, H[1H]−H[2H] = 2.12(14) Å), which is very short for two coordinate hydride atoms (in Cp_2NbH_3 the two closest hydrides lie 1.78(9) and 1.74(9) Å apart),[8c] but long for a dihydrogen molecule (the longest H−H bond distance found for H_2 coordinated molecules is 1.34(2) Å in the complex $[Os(\eta^2\text{-}H_2)(en)_2(CH_3)(CO_2)PF_6$ [22]). The coordination around the Au atom can be described as square-planar with a tetrahedral deformation (the dihedral angle between the planes H[1H]AuH[2H] and H[1H]′AuH[2H]′ is 23(5)°).

Discussion

The NMR observation of a quantum mechanical process in transition metal polyhydride complexes has appeared as one of the most astonishing phenomena in coordination chemistry. Attempts at modulating experimentally the exchange coupling values in order to determine the nature of the tunneling process have been briefly described by our group[12,14] and that of Heinekey.[10,13] However, this study gives us an unique opportunity to modulate the values of the couplings by different methods and gain information on the mechanism of this tunneling.

It is first of all clear that the modulation of the electron density on the metal as a result of the electron donating properties of the cyclopentadienyl ligands will greatly influence the magnitude of the exchange couplings. In mononuclear complexes such as **1**−**3**, we have related this electronic effect to the proximity of a thermally accessible dihydrogen state. This seemed at first sight much less clear for the Lewis acid adducts **7**−**14**.

Addition of a Lewis acidic coinage cation leads in each case to a 2:1 adduct which displays an AB_2 pattern for the hydrides and, with the exception of **7**, which shows evidence for the presence of exchange couplings.

The AB_2 pattern results from a fluxional process since at low temperature an ABC pattern is observed for the copper and gold adducts and a spectrum indicating a coalescence for the silver ones.

The energy of activation of the fluxional process which renders the two outer hydrides equivalent was estimated to 42−45 kJ·mol^{-1} in the case of copper adducts, 37 kJ·mol^{-1} for **11**, and near 40 kJ·mol^{-1} for the gold adducts (it was accurately measured as 38.7 kJ·mol^{-1} in the case of **14**). These numbers are comparable, but we can observe that copper adducts are less fluxional than gold ones which in turn are less fluxional than silver ones.

The effect of Lewis acid addition on the magnitude of exchange couplings is however much more important and does not follow the same order since addition of copper leads to a strong decrease of the observed H−H couplings, addition of silver does not change their order of magnitude, and addition of gold leads to a strong increase of the couplings.

In order to discuss these two experimental results, it is necessary to briefly consider the physical phenomena which could be at the origin of these anomalous couplings. In their first model Zilm, Heinekey et al. proposed that the existence of a low-frequency vibrational mode for the central hydride could be related to the occurrence of exchange couplings (see Introduction), whereas we proposed that the NMR properties of these trihydrides could result from rotational tunneling of dihydrogen in a slightly higher in energy dihydrogen state (Scheme 2a). The coordination of a Lewis acidic cation was expected to strongly perturbate the vibrational modes of niobium trihydrides and in particular the in-plane deformation.

This mode should shift at high frequency which in turn should inhibit the quantum mechanical exchange. This is obviously not the case for the gold adducts. In our alternative model, it is equally difficult at first sight to invoke the presence of a dihydrogen state. However, we propose an equilibrium between two isomeric forms as shown on Scheme 2b.

Scheme 2. Proposed Adducts for Explaining the Presence of Exchange Coupling in Niobocene Trihydrides and Their Lewis Acid Adducts

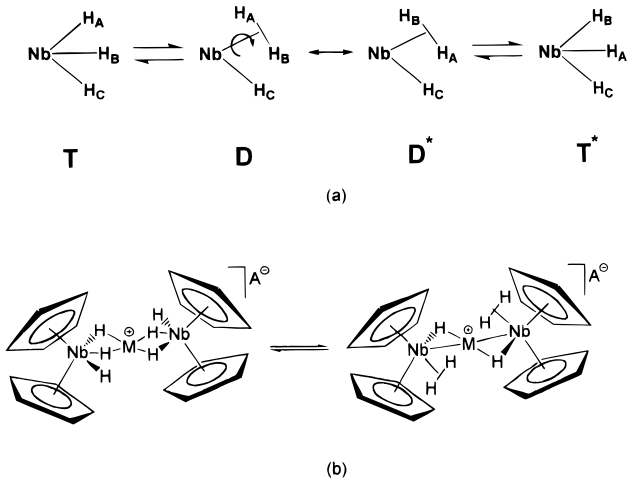

The dihydrogen form implies a linear coordination of the coinage cation to only two hydrogens. This seems surprising, but the X-ray crystal structure of **14** indicates the presence of two proximate hydrides and similar compounds in which H_2 has been substituted by CO have been isolated and the copper adduct has been characterized by an X-ray crystal structure.[24]

The difference in the magnitude of exchange couplings between the coinage elements could be explained as follows. That the presence of copper inhibits exchange couplings in **7**−**9** could arise from the stabilization of the dihydrido bridged form, which, in our opinion, could result from the good Lewis acidic character of the copper cation. Furthermore, a coordination number of 2, although not impossible, is unlikely for copper. When substituting copper by silver and gold, the presence of a more extended electronic cloud will render the coinage cations less acidic and therefore less strongly bound to the hydrides. This could explain both the higher classical fluxionality and the increase of exchange couplings for silver compared to copper. However, the very important increase in exchange couplings but lower fluxionality of the gold adducts compared to the silver ones looks anomalous. It results then probably from a stabilization of the dihydrogen form, perhaps through electron donation from the niobium III center to the gold cation. Such an interaction between the niobium doublet and gold has previously been shown to exist in a related niobium/gold raft cluster.[23]

The line shape analysis allows one to draw several conclusions. First, the solvent dependence is in agreement with a rearrangement of the molecule during the tunneling process.

An exponential fit of the temperature dependence on the 187−279 K range was calculated for compound **14** following the equation

$$J = J_0 + A_{bc} \exp[-E_{bc}/RT] \qquad (1)$$

This leads to the following parameters given in Table 3. In a first approach, it is tempting to consider J_0 as the temperature independent magnetic coupling constant. A value near 20 Hz

(24) Antiñolo, A.; Carrillo, F.; Chaudret, B.; Fajardo, M.; García-Yuste, S.; Lahoz, F. J.; Lanfranchi, M.; López, J. A.; Otero, A.; Pellinghelli, M. A. *Organometallics* **1995**, *14*, 1297.

Table 3

solvent	J_0 (Hz)	E_{bc} (kJ·mol^{-1})	A_{bc} (Hz)
THF-d_8	21.2	10.2 ± 0.8	34 700
$CDCl_2F/CDClF_2$	47.3	11.6 ± 1.2	19 300

is possible, but a value of 47.3 Hz seems too high. This is perhaps related to the fact that as stated before in this paper several conformers are present which could show a different temperature dependence. It would then be necessary to include not one but several exponential functions. The energy term in a single exponential function would be related to the difference in energy between the two isomeric states. This difference of energy is however close to the calculated values for systems not containing Lewis acids. Finally the preexponential factor A_{bc} would represent the pure exchange coupling constant.

Conclusion

We report in this study the preparation of a new series of substituted niobocene trihydrides and of their adducts with Lewis acidic coinage cations. We demonstrate first that exchange couplings present in the long studied Cp_2NbH_3 (**1**) can be suppressed upon addition of "Cu^+". A sharp temperature independent AB_2 spectrum is obtained which definitely rules out the presence of any factor other than exchange couplings to explain the line width, absence of couplings, and temperature dependence of the spectrum of **1**.

The second result is the demonstration that small electron density modifications on the ligands will induce a large modification of the exchange couplings magnitude, probably as a result of a modification of the trihydride/hydrido dihydrogen gap in agreement with our proposed model.

The most surprising and novel aspect of this work is however that addition of a coinage cation will in general not suppress the tunneling phenomenon but, in the case of gold adducts, will even lead to a very significant increase of exchange couplings. It is difficult in our opinion to explain these observations following a simple vibrational model.

In contrast, we propose a model implying an isomerization of the starting complex containing one terminal and two bridging hydrides into one containing one bridging hydride and one dihydrogen molecule. It is not possible at this stage to determine whether the dihydrogen isomer is a stable species (minimum on the energy surface) or only on the reaction path of the tunneling process.

In such a case the differences in the rate of the classical fluxional behavior between the three types of adducts can be explained by the stabilization of the dihydro bridged form in the case of copper and of the dihydrogen one in the case of gold. This last stabilization would explain the magnitude of exchange couplings found for the gold adducts.

Additional evidence for the existence of such a dihydrogen state comes from the isolation of a $[\{Nb(C_5H_4SiMe_3)_2(CO)\}_2(\mu\text{-}H)_2Cu]^+$ and of the solvent dependence of exchange couplings in a gold adduct which suggests a rearrangement of the complex.

Experimental Section

General Procedure. All manipulations were conducted under an inert atmosphere of dry nitrogen or argon with use of standard Schlenk tube techniques. Solvents were distilled from appropriate drying agents and degassed before use.

The salts $Cu(MeCN)_4PF_6$ [25] and $Au(THT)PF_6$, [26] THT = tetrahydrothiophene, and the complexes $Nb(C_5H_5)_2H_3$ [8d] and $Ta(C_5H_5)_2H_3$ [27] were prepared as described in the literature. $AgBF_4$ was purchased from Ventron and used without purification. Carbon and hydrogen microanalyses were performed with a Perkin-Elmer 2400 microanalyzer. Infrared spectra were recorded as Nujol mulls between CsI plates in the region 200−4000 cm^{-1} using a Perkin-Elmer 883 spectrophotometer. ^{1}H NMR spectra were recorded on Unity 300 Varian and Bruker WM 250 and 500 spectrometers, respectively. Probe temperatures were calibrated by comparison to the observed chemical shifts differences in the spectrum of pure methanol with use of the data reported by Van Geet.[28]

Preparation of $M(C_5H_3RR')_2H_3$, M = Nb, R = H, R′ = $SiMe_3$ (2); M = Nb, R = R′ = $SiMe_3$ (3); M = Ta, R = H, R′ = $SiMe_3$ (5); M = Ta, R = R′ = $SiMe_3$ (6). To a toluene (50 mL) suspension of $Nb(C_5H_4SiMe_3)_2Cl_2$ (1.18 g, 2.70 mmol) was added a solution of $Na[AlH_2(OCH_2CH_2OMe)_2]$ ("Red-Al") in toluene (2.73 g, 13.50 mmol). After stirring for $^1/_2$ h, a deep red solution was obtained which was hydrolized by adding 5 mL of oxygen-free water. Filtration of the precipitate of aluminium hydroxide, and removal of the solvent gave a light brown solid. It was recrystalized in ethanol to give air-sensitive white crystals of $Nb(C_5H_4SiMe_3)_2H_3$ (**2**).

Complexes **3**, **5**, and **6** were prepared in a similar way.

Compound 2. IR (Nujol): 1740 cm^{-1} (m) (Nb−H). ^{1}H NMR (C_6D_6, ppm, referenced to TMS): δ 4.88, 4.82 (m, 4H, C_5H_4), 0.22 (s, 9H, $SiMe_3$), −3.47 (m, 3H, NbH_3). Anal. Calcd for $C_{16}H_{29}Si_2Nb$: C, 51.87; H, 7.88. Found: C, 51.79; H, 7.93.

Compound 3. IR (Nujol): 1720 cm^{-1} (m, br) (Nb−H). ^{1}H NMR (C_6D_6, ppm, referenced to TMS): δ 5.06 (m, 3H, C_5H_3), 0.24 (s, 18H, $SiMe_3$), −4.19 (m, 3H, NbH_3). Anal. Calcd for $C_{22}H_{45}Si_4Nb$: C, 51.32; H, 8.80. Found: C, 51.25; H, 8.90.

Compound 5. IR (Nujol): 1760 cm^{-1} (m) (Ta−H). ^{1}H NMR (C_6D_6, ppm, referenced to TMS): δ 4.90, 4.70 (m, 4H, C_5H_4), 0.26 (s, 9H, $SiMe_3$), −2.13 (t, 1H, TaH; J_{H-H} 8.8Hz), −3.29 (d, 2H, TaH_2; J_{H-H} = 8.8Hz). Anal. Calcd for $C_{16}H_{29}Si_2Ta$: C, 41.92; H, 6.37. Found: C, 41.80; H, 6.42.

Compound 6. IR (Nujol): 1760 cm^{-1} (m, br) (Ta−H). ^{1}H NMR (C_6D_6, ppm, referenced to TMS): δ 5.11, 4.93 (m, 4H, C_5H_3), 0.21 (s, 18H, $SiMe_3$), −2.83 (t, 1H, TaH; J_{H-H} = 7.3Hz), −3.75 (d, 2H, TaH_2; J_{H-H} = 7.3Hz). Anal. Calcd for $C_{22}H_{45}Si_4Ta$: C, 43.83; H, 7.52. Found: C, 43.70; H, 7.63.

Preparation of $[\{Nb(C_5H_3RR')_2H_3\}_2Cu]PF_6$, R = R′ = H (7); R = H, R′ = $SiMe_3$ (8); R = R′ = $SiMe_3$ (9). $Nb(C_5H_5)_2H_3$ (0.20 g, 0.90 mmol) was dissolved in 20 mL of THF. $Cu(MeCN)_4PF_6$ (0.17 g, 0.45 mmol) was added at −78 °C affording, after 15 min of stirring at room temperature, a light green solution which was evaporated to dryness. The residue was extracted with a mixture of dichloromethane−hexane (1:3, 4 mL). Complex **7** was obtained on cooling as a white-brown crystalline solid (0.29 g, 97% yield).

Complexes **8** and **9** were also isolated as white crystalline solids in a similar way. Yields: **8**, 98%; **9**, 90%.

Compound 7. IR (Nujol): 1740 (m, br) (Nb−H), 840 (s, br) cm^{-1} (PF_6^-). ^{1}H NMR (CD_3COCD_3, ppm, referenced to TMS): 5.9 (20H, C_5H_5), −4.2 d, −6.2 t (6H, hydrides, AB_2). Anal. Calcd for $C_{20}H_{26}PNb_2CuF_6$ (**7**): C, 36.36; H, 3.91. Found: C, 36.90; H, 3.89.

Compound (8). IR (Nujol): 1750 (m, br) (Nb-H), 840 (s, br) cm^{-1} (PF_6^-). ^{1}H NMR (CD_3COCD_3, ppm, referenced to TMS): δ 5.30, 5.90 (16H, C_5H_4, AA′BB′, J_{H-H} = 2.4Hz); 0.30 (36H, $SiMe_3$), −3.90, −4.80 (6H, hydrides, AB_2). Anal. Calcd for $C_{32}H_{58}Si_4PNb_2CuF_6$ (**8**): C, 40.48; H, 6.11. Found: C, 40.28; H, 6.30.

Compound 9. IR (Nujol): 1720 (m, br) (Nb−H), 840 (s, br) cm^{-1} (PF_6^-). ^{1}H NMR (CD_3COCD_3, ppm, referenced to TMS): δ 5.59 (d, 8H), 4.94 (t, 4H, C_5H_3, J_{H-H} = 1.6Hz); 0.38 (72H, $SiMe_3$), −4.20, −5.10 (6H, hydrides, AB_2). Anal. Calcd for $C_{44}H_{90}Si_8PNb_2CuF_6$ (**9**): C, 42.71; H, 7.27. Found: C, 42.48; H, 7.31.

Preparation of $[\{Nb(C_5H_3RR')_2H_3\}_2Ag]BF_4$, R = H, R′ = $SiMe_3$ (10); R = R′ = $SiMe_3$ (11). To a solution of $Nb(C_5H_4SiMe_3)_2H_3$ (30.20 g, 0.50 mmol) in THF was added $AgBF_4$ (0.10 g, 0.25 mmol). After 15 min of stirring at room temperature, a brown solution was obtained which was evaporated to dryness. Complex **10** was isolated as a white or light brown microcrystalline solid by crystallization from tetrahydrofuran−diethyl ether (1:3, 4 mL) (0.24 g, 96% yield).

(25) Kubas, G. J. *Inorg. Synth.* **1979**, *19*, 90.
(26) Usón, R.; Laguna, A.; Laguna, M. *Inorg. Synth.* **1989**, *26*, 86.
(27) Green, M. H. L.; Mc Cleverty, J. A.; Patt, L.; Wilkinson, G. J. *J. Chem. Soc.* **1961**, 4854.
(28) Van Geet, A. L. *Anal. Chem.* **1968**, *40*, 2227.

Table 4. Crystallographic Data for Complex **14**·3THF

formula	$[C_{44}H_{90}AuNb_2Si_8]PF_6 \cdot 3C_4H_8O$
fw	1587.95
cryst syst	orthorhombic
space group	*Pbcn*
cell dimens	
a, Å	17.154(4)
b, Å	20.137(5)
c, Å	22.973(6)
V, Å^3	7936(3)
Z	4
d_{calc}, g·cm^{-3}	1.329
μ, cm^{-1}	23.17
radiation (λ, Å)	Mo Kα (0.710 73)
2θ range, deg	6-54
scan type	$\theta/2\theta$
scan speed, deg·min^{-1}	3−10
cryst size, mm	0.15 × 0.18 × 0.24
collcn range	$+h,+k,+l$
no. of unique reflns	8635
no. of reflns used	3082 ($I \geq 2\sigma(I)$)
$R(F)$, $R_w(F)$[a]	0.0346, 0.0381
T, K	295

[a] $R = \sum||F_o| - |F_c||/\sum|F_o|$. $R_w = [\sum w(|F_o| - |F_c|)^2/\sum w(F_o)^2]^{1/2}$.

Complex **11** was obtained in a similar way (98% yield) as a white microcrystalline solid using $Nb(C_5H_3(SiMe_3)_2)_2H_3$. All attempts to isolate the adduct using the complex $Nb(C_5H_5)_2H_3$ were unsuccessful, because the products descompose in all of the operation conditions.

Compound 10. IR (Nujol): 1780 (m, br) (Nb−H), 1250 (s) cm^{-1} (BF_4^-). ^{1}H NMR (CD_3COCD_3, ppm, referenced to TMS): δ 5.20, 5.80 (16H, C_5H_4, AA′BB′, J_{H-H} = 2.4Hz); 0.28 (36H, $SiMe_3$), −3.70 (6H, hydrides, AB_2). Anal. Calcd for $C_{32}H_{58}Si_4BNb_2AgF_4$ (**10**): C, 41.07; H, 6.20. Found: C, 41.11; H, 6.30.

Compound 11. IR (Nujol): 1760 (m, br) (Nb−H), 1250 (s) cm^{-1} (BF_4^-). ^{1}H NMR (CD_3COCD_3, ppm, referenced to TMS): δ 4.70, 5.50 (12H, C_5H_3), 0.34 (72H, $SiMe_3$), −3.60, −4.10 (6H, hydrides, AB_2). Anal. Calcd for $C_{44}H_{90}Si_8BNb_2AgF_4$ (**11**): C, 43.17; H, 7.36. Found: C, 43.10; H, 7.40.

Preparation of [{Nb(C$_5$H$_3$RR′)$_2$H$_3$}$_2$Au]PF$_6$, R = R′ = H (12); R = H, R′ = SiMe$_3$ (13); R = R′ = SiMe$_3$ (14). A THF solution (5 mL) of Au(THT)PF_6 (0.45 mmol) was prepared "in situ" by reaction (15 min) of Au(THT)Cl (0.14 g, 0.45 mmol) with $TlPF_6$ (0.16 g, 0.45 mmol); the white precipitate (TlCl) was separated by filtration and was added to a THF solution (20 mL) of $Nb(C_5H_5)_2H_3$ (0.20 g, 0.9 mmol) at −78 °C. After 15 min of stirring at room temperature, an orange solution was obtained. The solvent was pumped off and the residue extracted with a mixture of THF−diethyl ether (1:1). Complex **12** was obtained on cooling as a red microcrystalline solid (0.28 g, 80% yield).

Complexes **13** and **14** were obtained in a similar way as orange (**13**) and yellow-green (**14**) microcrystalline solids. Yields: **13**, 90%; **14**, 90%.

Compound 12. IR (Nujol): 840 cm^{-1} (s, br) (PF_6^-). ^{1}H NMR (CD_3COCD_3, ppm, reference TMS): δ 6.00 (20H, C_5H_5), −0.40···−2.20 (6H, hydrides, AB_2, see text). Anal. Calcd for $C_{20}H_{26}PNb_2AuF_6$ (**12**): C, 30.21; H, 3.27. Found: C, 30.27; H, 3.29.

Compound 13. IR (Nujol): 840 cm^{-1} (s, br) (PF_6^-). ^{1}H NMR (CD_3COCD_3, ppm, referenced to TMS): δ 5.30, 5.70 (16H, C_5H_4, AA′BB′, J_{H-H} = 2.4 Hz), 0.29 (36H, $SiMe_3$), +0.10···−1.70 (6H, hydrides, AB_2, see text). Anal. Calcd for $C_{32}H_{58}Si_4PNb_2AuF_6$ (**13**): C, 35.48; H, 5.36. Found: C, 35.61; H, 5.40.

Compound 14. IR (Nujol): 840 cm^{-1} (s, br) (PF_6^-). ^{1}H NMR (CD_3COCD_3, ppm, referenced to TMS): δ 4.70, 5.50 (12H, C_5H_3), 0.36 (72H, $SiMe_3$), −0.70···−1.70(6H, hydrides, AB_2, see text). Anal. Calcd for $C_{44}H_{90}Si_8PNb_2AuF_6$ (**14**): C, 38.50; H, 6.59. Found: C, 38.40; H, 6.70.

X-ray Data Collection, Structure Determination, and Refinement for 14. A single crystal of **14** was sealed in a Lindemann capillary under dry nitrogen and used for data collection. The crystallographic data are summarized in Table 4. Unit cell parameters were determined from the θ values of 30 carefully centered reflections having 10 < θ < 20°; data were collected at room temperature (22 °C) on a Phillips PW 1100 diffractometer, using the graphite monochromated Mo Kα radiation. All reflections with θ in the range 3−27° were measured; of 8635 independent reflections, 3082, having $I \geq 2\sigma(I)$, were considered observed and used in the analysis. The individual profiles were analyzed according to the technique of Lehmann and Larsen.[29] Intensities were corrected for Lorenz and polarization effects. No correction for absorption was applied. Only the observed reflections were used in the structure solution and refinement. The structure was solved by Patterson (SHELXS-86)[30] and Fourier methods and refined by full-matrix least-squares technique (SHELX-76),[30] first with isotropic and then with anisotropic thermal parameters in the last cycles for all non-hydrogen atoms of the cation and for the P atom of the anion. The hydride H atoms were clearly located in the ΔF map and refined isotropically. The positional parameters were tested by means of a "potential energy" technique, using the HYDEX program.[31] The H atoms of the Cp rings were located but not refined, with a fixed overall isotropic thermal parameter of 0.1 Å^2, while the H atoms of the Me groups were placed at their geometrically calculated positions and refined "riding" (d (C−H) = 0.96 Å) on the corresponding carbon atoms with a fixed overall isotropic thermal parameter. The F atoms of the PF_6 anion, with the P atom lying on a crystallographic 2-fold axis, were found disordered and located in two positions with an occupancy factor of 0.5. The THF molecules were found to be disordered, and no attempt was made to obtain satisfactory images; all of the atoms were treated as C atoms with an occupancy factor of 0.5. The final cycles of refinement were carried out on the basis of 327 variables; after the last cycles, no parameters shifted by more than 0.85 esd. The largest remaining peak in the final difference map was equivalent to about 0.57 e/Å^3. In the final cycles of refinement better results were obtained with unit weight. The atomic scattering factors, corrected for the real and imaginary parts of anomalous dispersion, were taken from ref 32. All calculations were carried out on the GOULD POWERNODE 6040 computer and on the ENCORE 91 of the Centro di Studio per la Strutturistica Diffractometrica del CNR, Parma, Italy. The final atomic coordinates and isotropic or equivalent thermal parameters for the non-hydrogen atoms are given in Table 4. The programs PARST[33] and ORTEP[34] were also used. A second crystal was previously examined with the same results. Unit cell parameters were determined from the θ values of 31 centered reflections having 10° < θ < 19°; data were collected at room temperature (22 °C) on a Siemens AED diffractometer, using the graphite monochromated MoKα radiation. All reflections with θ in the range 3−30° were measured; of 12508 measured reflections, 3986 having $I \geq 2\sigma(I)$, were considered observed and used in the analysis.

Acknowledgment. A.A., F.C.-H., M.F., J.F.-B., and A.O. gratefully acknowledge financial support from the DGICyT (Grant. No. PB 92-0715) of Spain. M.L. and M.A.P. gratefully acknowledge financial support from the Ministero dell'Università e della Ricerca Scientifica e Tecnologica (MURST) and the Consiglio Nazionale della Ricerca (CNR) (Rome, Italy).

Supporting Information Available: Tables of hydrogen atom coordinates and isotropic thermal parameters, anisotropic thermal parameters for the non-hydrogen atoms, complete bond distances and angles, least-squares planes, and crystallographic data (13 pages). Ordering information is given on any current masthead page.

IC960582E

(29) Lehmann, M. S.; Larsen, F. K. *Acta Crystallogr., Sect. A* **1974**, *30*, 580.
(30) Sheldrick, G. M. *SHELX-76*, Program for crystal structure determination; University of Cambridge: Cambridge England, 1976; *SHELXS-86*, Program for the solution of crystal structures; University of Gottingen: Gottingen, Germany, 1986.
(31) Orpen, A. G. *J. Chem. Soc., Dalton Trans.* **1980**, 2509.
(32) *International Tables for X-ray Crystallography*; Kynock Press: Birmingham, England, 1974; Vol. IV.
(33) Nardelli, M. *Comput. Chem.* **1983**, *7*, 95.
(34) Johnson, C. K. *ORTEP*, A fortran thermal-ellipsoid plot program for crystall structure illustrations; Report ORNL-3794 revised; Oak Ridge National Laboratory: Oak Ridge, TN, 1965.